

Properties of bilayer graphene-like Si_2C_{14} semiconductor using first-principle calculations

Nzar Rauf Abdullah

the date of receipt and acceptance should be inserted later

Abstract We theoretically investigate silicon doped bilayer graphene, Si-BLG, with different stoichiometry of Si-BLG structures. The dangling bonds of C-Si atoms are found at low concentration ratio of Si atoms inducing sp^3 -hybridization of buckled pattern in the structure. The Si-BLG with dangling bonds reveal strong mechanical response at low strain of a uniaxial load, and the fracture strain is seen at low strain ratio. The sp^3 -hybridization forms a small bandgap which induces an intermediate thermal and optical response of the system. In contrast, at higher Si concentration ratio, the Young modulus and fracture strain are increased comparing to the low Si concentration ratio. This is due to presence of high number of C-Si bonds which have a high tolerant under uniaxial load. In addition, a relatively larger bandgap or an overlap between valence and conduction bands are found depending on the Si configurations. In the presence of gaped Si-BLG, the thermal and optical response are high. We thus obtain a high Seebeck coefficient and a figure of merit with low electronic thermal conductivity which are useful for thermoelectric nanodevices, and an enhancement of optical response is acquired with a redshift in the visible range.

Nzar Rauf Abdullah
Division of Computational Nanoscience, Physics Department,
College of Science, University of Sulaimani, Sulaimani 46001,
Kurdistan Region, Iraq
Computer Engineering Department, College of Engineering,
Komar University of Science and Technology, Sulaimani
46001, Kurdistan Region, Iraq
Science Institute, University of Iceland, Dunhaga 3, IS-107
Reykjavik, Iceland Tel.: +770 144 3854
E-mail: nzar.r.abdullah@gmail.com

1 Introduction

The ability to fabricate of monolayer graphene [1] leads researchers to study quantum Hall effect plateaus that is explained in terms of Dirac-like chiral quasiparticles with Berry phase π . Consequently, bilayer graphene (BLG) has been considered as one of the interested structure of study [2, 3]. One of the interested feature of BLG is the possibility to locally induce a bandgap and tune its magnitude by applying a strong electric field perpendicular to the carbon nanosheets [4–7]. This property of BLG can be used to design next-generation transistors that would work faster and use less energy [8, 9].

The physical properties such as the bandgap of BLG can also be tuned by doping of foreign atoms [10, 11]. Several foreign atoms have been used to improve physical properties of monolayer and bilayer graphene such as Boron/Nitrogen (B/N) atoms [11–14], cesium (Cs) [15, 16], Silicon (Si) atom [17, 18], and transition metals [19]. The BLG with B/N doping exhibits a semiconducting material with a small bandgap, where the Fermi energy is located in the bandgap [20, 21] which can be used to study photocatalysis [22]. The tuning bandgap by Si doped BLG have been reported and shown that the Si atoms induces a small bandgap due to the similar valence electron of Si and C atoms [17, 23]. The sandwiching a graphene by Cs induces thermodynamically stable flat band materials [24]. In the transition metals doped BLG, the electronic and magnetic properties as a function of strain have been also analyzed to indicate that the strain is important for the stabilities of the high-coverage TM-intercalated BLG [19, 25–27]. The bandgap tuning of BLG can thus improve the electrical, the thermal and the optical conductivities and modulate the mechanical properties [28].

The Si doping monolayer graphene has been investigated by several research groups. The Si atoms influences mechanical property such as Young's modulus of monolayer graphene, the optical [29] and thermal [30–33] characteristics. But the electronic, mechanical, thermal, and optical properties of Si-doped BLG have not been systematically investigated. In this work, we consider Si-doped AA-stacked BLG represented by SiC_{15} , and Si_2C_{14} structures depending on Si concentrations. The electronic, mechanical, optical and thermal characteristics are investigated using density functional theory. A comparison for different Si atoms configuration in BLG will be shown with detailed mechanisms of improving the BLG structures by Si impurity atoms [34–37].

In Sec. 2 the structure of BLG is briefly over-viewed. In Sec. 3 the main achieved results are analyzed. In Sec. 4 the conclusion of the results is presented.

2 Computational details

The calculations performed in this study are using DFT within Generalized Gradient Approximation (GGA) [38] and the computer software is Quantum Espresso (QE) package [39]. The calculations are also carried out on a 2×2 bilayer supercell arrangement with plane-wave basis set of Perdew-Burke-Ernzerhof (PBE) pseudopotentials [40] with 1088.45 eV cutoff-energy. Under the GGA-PBE, the van der Waals interactions between the layers of system is almost ignored. The structure relaxation is performed using the k -point grid is $12 \times 12 \times 1$ and the force on each atom is less than 10^{-6} eV/Å. For the Brillouin zone sampling and the calculations of the density of state (DOS), a $12 \times 12 \times 1$ and a $77 \times 77 \times 1$ grids are used, respectively.

The XCrySDen, crystalline and molecular structure visualization program, is utilized to visualize our structures [3, 41, 42]. Furthermore, the thermoelectric properties of the systems are investigated using the Boltzmann transport software package (BoltzTraP) [43]. The BoltzTraP code uses a mesh of band energies and has an interface to the QE package [44, 45]. The optical properties of the systems are obtained by the QE code with the broadening of 0.5 eV.

3 Results

In this section, we show the results of structural stability, electronic, mechanical, thermal, and optical properties of the Si-BLG with different concentration

and configurations of Si atoms in a 2×2 bilayer supercell [46].

3.1 Model

In Fig. 1 the pristine BLG (a) and Si-BLG (b-d) structure are presented. We consider one Si atom is doped in the top layer with the doping concentration ratio of 6.25% identifying as SiC_{15} (b). The vertical gray lines indicate the border of 2×2 supercell [47]. In addition, we also assume two Si atoms doped in BLG with doping concentration ratio of 12.5% in two configurations of Si atoms: First, both Si atoms are doped in the top layer at the para-positions identifying as Si_2C_{14} -I (c). Second, one Si atom is doped at the para-position of the top layer and another Si atom is put at meta-position of the bottom layer called Si_2C_{14} -II (d). We avoid the formation of Si-Si bonds in the Si-BLG, which substantially destabilize the hexagonal system [48].

The interlayer distance, lattice constant, and the C-C bond length of pristine BLG are found to be 4.64, 2.46, 1.42 Å, respectively, which are expected for the GGA-PBE calculations. But if the van der Waals interactions in the exchange (XC) functional with LDA is included, the interlayer distance becomes 3.6 Å, which is close to experimental work [49–52]. The interlayer distance for all three Si-BLG structures is 4.64 Å which is almost unchanged indicating no interlayer interaction energy due to Si atoms. This is opposite to the interlayer repulsive interaction between the Si-Si atoms in BLG which is recently observed when the LDA exchange correlation is assumed [53, 54].

Another point is that the Si atom in top layer of SiC_{15} is moved towards the bottom layer with 0.7 Å away from the top layer. This deviation of Si atoms from graphene surface has been reported with same deviation length, 0.7 Å [17, 55]. The Si shifting here forms the dangling bonds of Si-C in which the Si atom tends to adopt sp^3 hybridization, such as in silicene where the buckled pattern forms. It thus increases the C-Si bond length to 1.71 Å and slightly increase the average C-C bond lengths to 1.45 Å. This shifting of the Si atom will influence the physical properties of the system as it will be shown later.

In the Si_2C_{14} -I, the average C-C bond length in the top(bottom) layer is 1.37(1.53) Å, and the C-Si bond length is 1.69 Å. In the case of Si_2C_{14} -II, the average C-C bond length in the top(bottom) layer is 1.47(1.5) Å, and the C-Si bond length is 1.68 Å. It can be clearly seen that the position of Si atoms in the hexagonal structure of graphene influence the bond length and thus the physical properties of the systems [56–58].

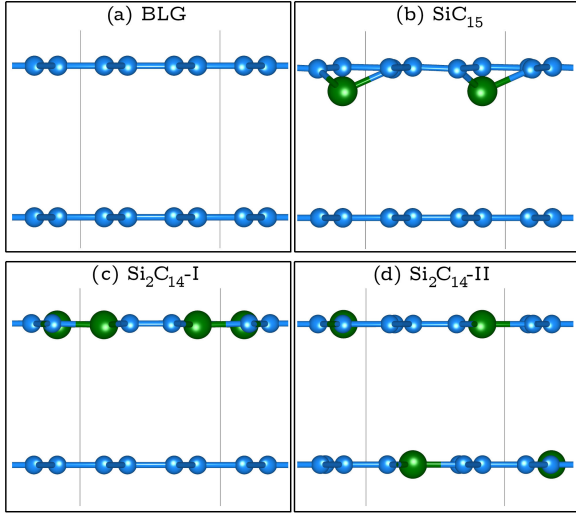


Fig. 1: AA-stacked pristine BLG (a), SiC_{15} (b), Si_2C_{14} -I (c), and Si_2C_{14} -II (d). The C and Si atoms are blue and green colors, respectively.

3.2 Mechanical response

The modifications of bond lengths and the Si-BLG structures affect the mechanical properties of the system. The stress-strain curves for pristine BLG (gray), SiC_{15} (green), Si_2C_{14} -I (blue), and Si_2C_{14} -II (red) in the zigzag (a) and armchair (b) directions are shown in Fig. 2. In 2D materials, the two basis vectors are perpendicular to each other. We therefore apply uniaxial strains directly along the vector direction. Tension simulation is carried out by imposing in-plane tensile strain at a rate of 0.02 per step in the uniaxial zigzag or armchair direction.

The stress-strain curves of pristine BLG are consistent with those existing in the literature for both zigzag and armchair directions, showing the reliability of our calculations [59]. Similar to previous investigations, the pristine BLG obeys linear relationships within a small strain range up to 5%. The linear elastic region gives the Young modulus of 974 GPa which is very close to experimental value [60]. In addition, the ultimate strength of pristine BLG is 99.64 GPa (zigzag) and 96.22 GPa (armchair) at a strain of 0.151 and 0.126, respectively. Since there is no stretching in the pristine BLG after the fracture strain, the values of ultimate stress are also equal to the fracture strain. This slightly anisotropy of the ultimate stress in zigzag and armchair directions has also been observed for pristine monolayer graphene [61].

In the Si-BLG structures, it is interesting to see that linear elastic region and ultimate strength for SiC_{15} are decreased in both zigzag and armchair directions. The reduction is much stronger in the zigzag direction

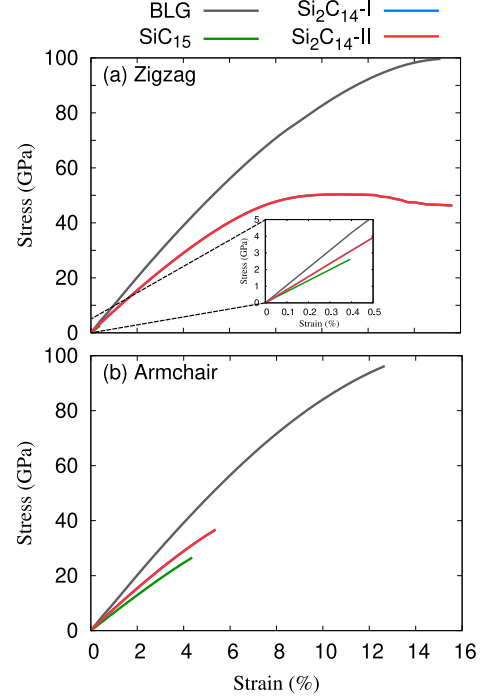


Fig. 2: Stress-strain curves for pristine BLG (gray), SiC_{15} (green), Si_2C_{14} -I (blue), and Si_2C_{14} -II (red) in the zigzag (a) and armchair (b) directions.

(see Fig. 2(inset)). The ultimate strength is 3.8 GPa with strain 0.4% in the zigzag direction, and 26.58 GPa at strain 4.3% in the armchair direction. This is attributed to the dangling bonds of Si-C in which the Si atom tends to adopt sp^3 hybridization. In addition, the moving out of Si atom introduces extremely unbalanced bonds strength which distorts the perfect hexagon rings of the 2×2 supercell honeycomb. Consequently, the pre-elongated C-C and Si-C bonds of SiC_{15} under the uniaxial tension are lifted.

One also can clearly see that the stress-strain curves for both Si_2C_{14} -I, and Si_2C_{14} -II in the zigzag and armchair directions are irrespective of doping configurations, and they are the same because number of Si-C bonds are equal with different configurations in both structures. The Young modulus and tensile or ultimate strength are found to be 732(728), and 50.22(36.72) for the zigzag/armchair directions, respectively. The reduction of stress-strain curves for Si_2C_{14} -I, and Si_2C_{14} -II refers to the presence of more Si-C bonds in these structures. In addition, the ultimate strength and fracture strain in the zigzag direction is higher than that of the armchair which is due to existing of more Si-C bonds in the zigzag direction. This is because in the Si-C bonding the charge distribution of the Si atom is more easily reshaped than that of the C atom as the

Si atom has much lower electronegativity. It arises Si-C bonds much more tolerance of the stretched process.

3.3 Band energy and DOS

The electronic band structures and the DOS of pristine BLG (a) and Si-BLG (b-d) are shown in Fig. 3, and Fig. 4, respectively. The linear dispersion of the first valence band, π , and the conduction band, π^* , of the pristine BLG is found with zero bandgap and DOS. The energy spacing between the π_2 - π_1 (π_2^* - π_1^*) is almost 0.11 eV [62]. The linear dispersion of pristine BLG band structure around the Fermi level shows the semimetallic nature where valence band maxima (π band) and the conduction band minima (π^* band) touch each other only at the high symmetry K point. The Hamiltonian that defines the electronic structure of pristine BLG around the Dirac point can be given as [63]

$$\hat{H} = \begin{pmatrix} \Delta & \hbar v_F(k_x - ik_y) \\ \hbar v_F(k_x + ik_y) & -\Delta \end{pmatrix} \quad (1)$$

where, Δ , v_F , and k indicate onsite energy difference between the C atoms located at A and B sites, Fermi velocity, and momentum of charge carriers. The linear relation refers to the zero value of the onsite energy difference, Δ , in pristine BLG arising from the presence of inversion symmetry in pristine BLG. The zero value of onsite energy difference refers to the potentials seen by the C atoms at the sites A and B are the same. Consequently, there is no opening up of energy gap in monolayer and bilayer graphene.

In the Si-BLG, the overall energy spacing between π and π^* at M-point determining the interlayer interaction is not much changed because the GGA-PBE is assumed where the interlayer interaction is ignored. But a strong influence between π and π^* at Γ -point is seen inflecting the optical transitions [45, 46, 64]. The bandgap of SiC₁₅ and Si₂C₁₄-II are found to be 0.11 and 0.67 eV exhibiting semiconducting materials. The small bandgap of Si doped graphene may refer to the same number of the valence electron of Si and C atoms. In general, a band gap is opened near the K point due to breaking of the inversion symmetry by the distortion generated by the Si atoms configuration. The reason for the broken symmetry is that the potential seen by the atoms at sites A and B is now different, leading to a finite value of onsite energy $\Delta \neq 0$, where $\Delta = \alpha(V_A - V_B)$ with α being a constant value and V_A (V_B) is the potential seen by an atom at the site A(B) [65]. Furthermore, a small overlap of valence and conduction bands of Si₂C₁₄-I indicate a metallic

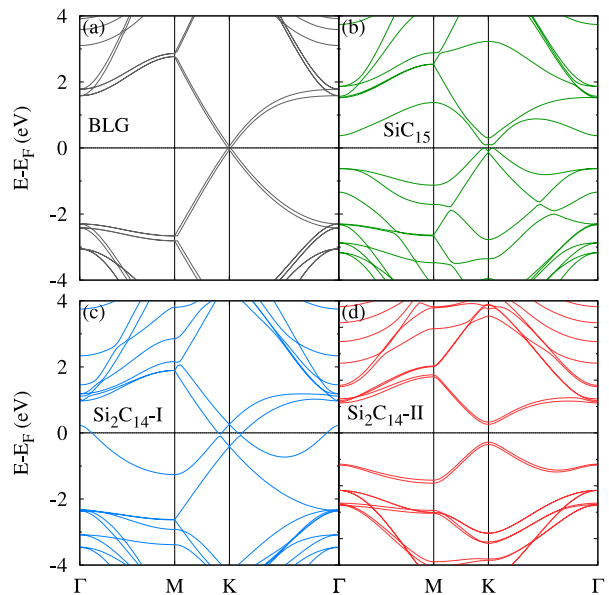


Fig. 3: Electronic band structure of pristine BLG (a), SiC₁₅ (b), Si₂C₁₄-I (c), and Si₂C₁₄-II (d).

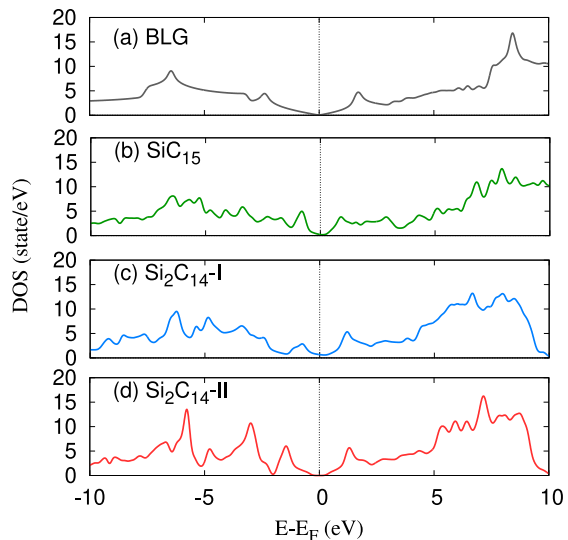


Fig. 4: Density of state of pristine BLG (a), SiC₁₅ (b), Si₂C₁₄-I (c), and Si₂C₁₄-II (d).

behavior of this structure. These modifications in electronic band structure and induced bandgap will effectively change the thermal properties of the systems.

3.4 Thermal response

The thermal properties such as Seebeck coefficient (a), figure of merit (b), electronic thermal conductivity (c), and specific heat (d) at temperature $T = 100$ K are shown in Fig. 5 for the pristine BLG and Si-BLG structures [66–68]. We are interested in thermal behavior of

the systems at low temperature and it has been reported that the electrons and phonons thermal behaviors are decoupled at low temperature range from 20 to 160 K [69]. We thus present the electronic part of thermal properties.

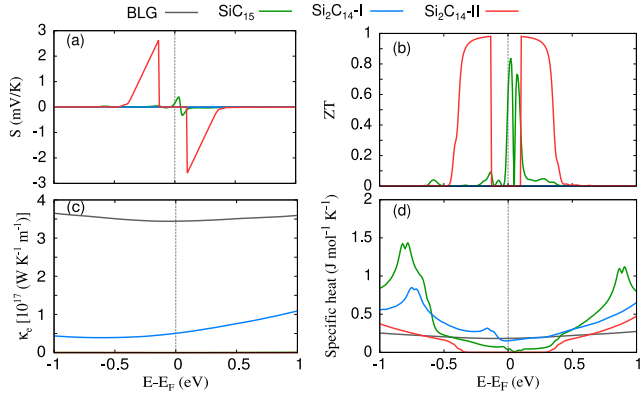


Fig. 5: Seebeck coefficient, S , (a), Figure of merit, ZT , (b), electronic thermal conductivity, κ_e , (c), and specific heat (d) at $T = 100$ K for pristine BLG (gray), SiC_{15} (green), Si_2C_{14} -I (blue), and Si_2C_{14} -II (red).

The S and the ZT of pristine BLG and Si_2C_{14} -I are very small due to the zero bandgap and overlapping the valence and conduction bands, respectively. This is attributed to the cancellation effect from electron-hole contributions to the transport quantities. So, the highest thermal conductivity and specific heat are thus found around the Fermi energy for these two structures. In contrast, opening up the bandgap of SiC_{15} and Si_2C_{14} -II maximizes the S , and ZT and minimizes the thermal conductivity and specific heat around the Fermi energy. Therefore, the maximum S and ZT are found for Si_2C_{14} -II as it has the maximum bandgap among these structures.

3.5 Optical response

The modified electronic band structures and DOSs due to Si dopants are expected to tune the optical response of BLG. The optical response of the Si-BLG under applied in- (left panel) and out-plane (right panel) electric fields is demonstrated in Fig. 6, where the imaginary part of dielectric function (a-b), the absorption coefficient (c-d), and the Reflectivity, R , (e-f) of pristine BLG and Si-BLG are presented.

In the case of pristine BLG, two main peaks in the imaginary dielectric function are observed at 3.95 eV corresponding to the π to π^* transition and at 13.87 eV

generated due to the σ to σ^* transition when an in-plane electric field is applied, E_{in} . In the case of out-plane applied electric field, E_{out} , the two main peak are formed by transitions from the σ to π^* at 11.22 eV and the π to σ^* at 14.26 eV. These transitions are in a good agreement with literature [70–72]. The absorption coefficient is related to the imaginary part of dielectric function. The absorption coefficient of pristine BLG shows two obvious peaks at 4.41 and 14.35 eV for E_{in} , and two peaks at 11.78 and 14.67 eV for E_{out} . In addition, it is noticed that two peaks in reflectivity of pristine BLG are found at 4.32 and 15.55 eV for E_{in} with almost the same intensity, and two peaks at 11.22, and 15.31 eV for E_{out} with different intensities. It should be mentioned that the peak positions of pristine BLG are strongly dependent on the interlayer distance [70, 73]. The peak intensity of ϵ_2 , α , and R here in both E_{in} and E_{out} directions are quite similar to previous studies when the interlayer distance is close to 4.64 Å, as it is considered in our work. It is also seen that the optical response of pristine BLG becomes insignificant beyond the energy or optical frequency of ≈ 25 eV irrespective of polarization state [74].

The optical response of Si-BLG is significantly modulated because the band structure and the DOS are changed. The frequency dependent variation of ϵ_2 for SiC_{15} and Si_2C_{14} -II is enhanced in both directions of applied electric fields especially at the low energy range. This is attributed to the opening up bandgap of these two structures. A new peak in ϵ_2 at 0.9 eV for Si_2C_{14} -II is observed in the E_{in} direction referring to the existing a relatively larger bandgap. Another peak in ϵ_2 at 1.75 eV for SiC_{15} in the E_{out} direction is seen, which is due to decreasing the energy spacing between σ and π bands at the Γ -point allowing transition between these two bands at lower energy. In addition, a red shift in the peaks positions of these two structures occur in both directions of applied electric field arising again from the opening bandgap and significant changes in the DOS. Consequently, the red-shift in absorption spectra and Reflectivity have also been noticed.

In contrast, the optical response of Si_2C_{14} -I is reduced. For instant, the imaginary part of dielectric function absorption coefficient are significantly reduced. This reduction may refer to the overlapping of valence band maxima and conduction band minima at K - and Γ -points. As a result, the reflectivity is enhanced in both directions of applied electric field. It should be noticed that there peaks positions are almost unchanged here. The controlling of optical response by dopant atoms may be interested in opto-electronic devices.

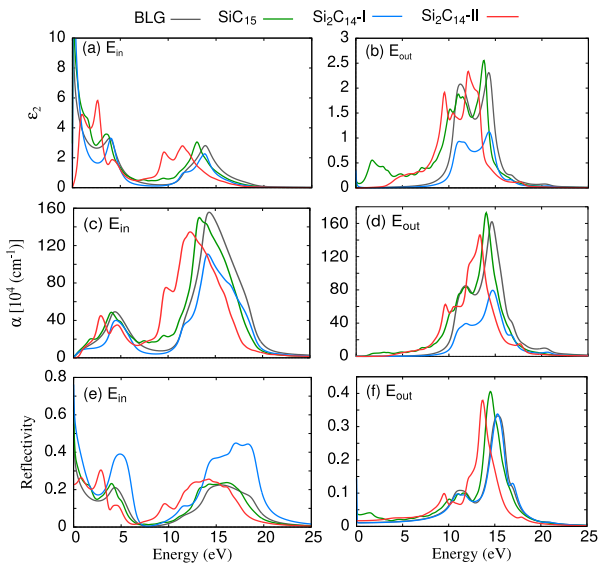


Fig. 6: Imaginary part of dielectric function, ϵ_2 , (a-b), absorption coefficient, α , (c-d), and Reflectivity (e-f) of pristine and Si-BLG for in-plane (left panel) and out-plane (right panel) of an applied electric fields.

4 Conclusion

To conclude, the first principles DFT technique is employed to compute the structural, electronic, mechanical, thermal, and optical properties of Si-BLG. It is observed that tuning the concentration ratio of Si dopant atoms with different configurations, the physical properties of the structures can be modulated. At low ratio of Si atoms doped in BLG, a modification in s and p orbitals hybridization is seen leading to a strong fracture strain at low strain ratio. These structures show a weak behavior of mechanical response. Furthermore, a small bandgap induced at low Si dopant atoms arises an intermediate Seebeck coefficient, figure of merit, and absorption coefficient. Increasing the ratio of Si dopant atoms when the Si atoms are doped in both layers of the BLG, a stronger mechanical response of Si-BLG is obtained in which the fracture strain is noticed at high strain. In addition, a larger bandgap due to higher ratio of Si dopant enhances thermal and optical responses of the system. If the Si dopant atoms is doped in only one layer, the valence and conduction bands are overlapped revealing low thermal and optical behaviors. Our present theoretical work might help to understand some thermal and optical properties of nano structured materials and to design nano optoelectronic devices involving graphene nano structures.

5 Acknowledgment

This work was financially supported by the University of Sulaimani and the Research center of Komar University of Science and Technology. The computations were performed on resources provided by the Division of Computational Nanoscience at the University of Sulaimani.

References

1. K. S. Novoselov, A. K. Geim, S. V. Morozov, D. Jiang, Y. Zhang, S. V. Dubonos, I. V. Grigorieva, and A. A. Firsov. Electric field effect in atomically thin carbon films. *Science*, 306(5696):666–669, 2004. ISSN 0036-8075. doi: 10.1126/science.1102896. URL <https://science.sciencemag.org/content/306/5696/666>.
2. Edward McCann, David S.L. Abergel, and Vladimir I. Fal'ko. Electrons in bilayer graphene. *Solid State Communications*, 143(1):110–115, 2007. ISSN 0038-1098. doi: 10.1016/j.ssc.2007.03.054. URL <http://www.sciencedirect.com/science/article/pii/S0038109807002918>. Exploring graphene.
3. N R Abdullah, C S Tang, A Manolescu, and V Gudmundsson. Electron transport through a quantum dot assisted by cavity photons. *Journal of Physics:Condensed Matter*, 25:465302, 2013.
4. Kaoru Kanayama and Kosuke Nagashio. Gap state analysis in electric-field-induced band gap for bilayer graphene. *Scientific Reports*, 5(1):15789, Oct 2015. ISSN 2045-2322. doi: 10.1038/srep15789. URL <https://doi.org/10.1038/srep15789>.
5. Vishal Panchal, Cristina Giusca, Arseniy Lartsev, Rositsa Yakimova, and Olga Kazakova. Local electric field screening in bilayer graphene devices. *Frontiers in Physics*, 2:3, 2014. ISSN 2296-424X. doi: 10.3389/fphy.2014.00003. URL <https://www.frontiersin.org/article/10.3389/fphy.2014.00003>.
6. Vidar Gudmundsson, Nzar Rauf Abdullah, Anna Sitek, Hsi-Sheng Goan, Chi-Shung Tang, and Andrei Manolescu. Time-dependent current into and through multilevel parallel quantum dots in a photon cavity. *Phys. Rev. B*, 95:195307, May 2017. doi: 10.1103/PhysRevB.95.195307. URL <https://link.aps.org/doi/10.1103/PhysRevB.95.195307>.
7. Nzar Rauf Abdullah and Vidar Gudmundsson. Single-photon controlled thermospin transport in a resonant ring-cavity system. *Physica E: Low-dimensional Systems and Nanostructures*, 104:223–228, 2018. ISSN 1386-9477. doi: 10.1016/j.physe.2018.07.036. URL <http://www.sciencedirect.com/science/article/pii/S1386947718301838>.
8. F. W. Chen, H. Ilatikhameneh, G. Klimeck, R. Rahman, Tao Chu, and Zhihong Chen. Achieving a higher performance in bilayer graphene fet - strain engineering. In *2015 International Conference on Simulation of Semiconductor Processes and Devices (SISPAD)*, pages 177–181, 2015.
9. N. R. Abdullah. Magnetically and photonically tunable double waveguide inverter. *IEEE Journal of Quantum Electronics*, 52(12):1–6, 2016. doi: 10.1109/JQE.2016.2626080.
10. Wenjing Zhang, Cheng-Te Lin, Keng-Ku Liu, Teddy Tite, Ching-Yuan Su, Chung-Huai Chang, Yi-Hsien Lee, Chih-Wei Chu, Kung-Hwa Wei, Jer-Lai Kuo, and Lain-Jong Li. Opening an electrical band gap of bilayer graphene with molecular doping. *ACS Nano*, 5(9):7517–7524, 2011. doi: 10.1021/nn202463g. URL <https://doi.org/10.1021/nn202463g>. PMID: 21819152.
11. Nzar Rauf Abdullah, Hunar Omar Rashid, Chi-Shung Tang, Andrei Manolescu, and Vidar Gudmundsson. Modeling electronic, mechanical, optical and thermal properties of graphene-like bc6n materials: Role of prominent bn-bonds. *Physics Letters A*, 384(32):126807, 2020. ISSN 0375-9601. doi: <https://doi.org/10.1016/j.physleta.2020.126807>. URL <http://www.sciencedirect.com/science/article/pii/S0375960120306745>.
12. G.A. Nemnes, T.L. Mitran, A. Manolescu, and Daniela Dragoman. Electric field effect in boron and nitrogen doped graphene bilayers. *Computational Materials Science*, 155:175 – 179, 2018. ISSN 0927-0256. doi: <https://doi.org/10.1016/j.commatsci.2018.08.054>. URL <http://www.sciencedirect.com/science/article/pii/S0927025618305822>.
13. Tongwei Han, Ying Luo, and Chengyuan Wang. Effects of si, n and b doping on the mechanical properties of graphene sheets. *Acta Mechanica Solida Sinica*, 28(6):618 – 625, 2015.

- ISSN 0894-9166. doi: [https://doi.org/10.1016/S0894-9166\(16\)30003-9](https://doi.org/10.1016/S0894-9166(16)30003-9). URL <http://www.sciencedirect.com/science/article/pii/S0894916616300039>.
14. Nzar Rauf Abdullah, Hunar Omar Rashid, Mohammad T. Kareem, Chi-Shung Tang, Andrei Manolescu, and Vidar Gudmundsson. Effects of bonded and non-bonded b/n codoping of graphene on its stability, interaction energy, electronic structure, and power factor. *Physics Letters A*, 384(12):126350, 2020. ISSN 0375-9601. doi: 10.1016/j.physleta.2020.126350. URL <http://www.sciencedirect.com/science/article/pii/S0375960120301602>.
 15. Niels Ehlen, Martin Hell, Giovanni Marini, Eddwi Hesky Hasdeo, Riichiro Saito, Yannic Falke, Mark Oliver Goerbig, Giovanni Di Santo, Luca Petaccia, Gianni Profeta, and Alexander Grüneis. Origin of the flat band in heavily cs-doped graphene. *ACS Nano*, 14(1):1055–1069, 2020. doi: 10.1021/acsnano.9b08622. URL <https://doi.org/10.1021/acsnano.9b08622>. PMID: 31825586.
 16. Nzar Rauf Abdullah, Chi-Shung Tang, Andrei Manolescu, and Vidar Gudmundsson. Thermoelectric inversion in a resonant quantum dot-cavity system in the steady-state regime. *Nanomaterials*, 9(5):741, 2019.
 17. Pablo A. Denis. Band gap opening of monolayer and bilayer graphene doped with aluminium, silicon, phosphorus, and sulfur. *Chemical Physics Letters*, 492(4):251–257, 2010. ISSN 0009-2614. doi: 10.1016/j.cplett.2010.04.038. URL <http://www.sciencedirect.com/science/article/pii/S0009261410005610>.
 18. Nzar Rauf Abdullah, Chi-Shung Tang, Andrei Manolescu, and Vidar Gudmundsson. Optical switching of electron transport in a waveguide-qed system. *Physica E: Low-dimensional Systems and Nanostructures*, 84:280 – 284, 2016. ISSN 1386-9477. doi: <https://doi.org/10.1016/j.physe.2016.06.023>. URL <http://www.sciencedirect.com/science/article/pii/S1386947716306749>.
 19. Ji-Hai Liao, Yu-Jun Zhao, Jia-Jun Tang, Xiao-Bao Yang, and Hu Xu. High-coverage stable structures of 3d transition metal intercalated bilayer graphene. *Phys. Chem. Chem. Phys.*, 18:14244–14251, 2016. doi: 10.1039/C6CP01841F. URL <http://dx.doi.org/10.1039/C6CP01841F>.
 20. L. S. Panchakarla, K. S. Subrahmanyam, S. K. Saha, Achutharao Govindaraj, H. R. Krishnamurthy, U. V. Waghmare, and C. N. R. Rao. Synthesis, structure, and properties of boron- and nitrogen-doped graphene. *Advanced Materials*, 21(46):4726–4730, 2009. doi: 10.1002/adma.200901285. URL <https://onlinelibrary.wiley.com/doi/abs/10.1002/adma.200901285>.
 21. Nzar Rauf Abdullah, Danyal A. Abdalla, Taha Y. Ahmed, Sarbast W. Abdulqadr, and Hunar Omar Rashid. Effect of bn dimers on the stability, electronic, and thermal properties of monolayer graphene. *Results in Physics*, 18:103282, 2020. ISSN 2211-3797. doi: <https://doi.org/10.1016/j.rinp.2020.103282>. URL <http://www.sciencedirect.com/science/article/pii/S2211379720317496>.
 22. Y. R. Tang, Y. Zhang, and J. X. Cao. Modulating the band gap of a boron nitride bilayer with an external electric field for photocatalyst. *Journal of Applied Physics*, 119(19):195303, 2016. doi: 10.1063/1.4950993. URL <https://doi.org/10.1063/1.4950993>.
 23. Vidar Gudmundsson, Hallmann Gestsson, Nzar Rauf Abdullah, Chi-Shung Tang, Andrei Manolescu, and Valeriu Moldoveanu. Coexisting spin and rabi oscillations at intermediate time regimes in electron transport through a photon cavity. *Beilstein Journal of Nanotechnology*, 10(1):606–616, 2019.
 24. I. Hase, T. Yanagisawa, and K. Kawashima. Computational design of flat-band material. *Nanoscale Research Letters*, 13(1):63, Feb 2018. ISSN 1556-276X. doi: 10.1186/s11671-018-2464-y. URL <https://doi.org/10.1186/s11671-018-2464-y>.
 25. Chi-Shung Tang, Jia-An Keng, Nzar Rauf Abdullah, and Vidar Gudmundsson. Spin magneto-transport in a rashba-dresselhaus quantum channel with single and double finger gates. *Physics Letters A*, 381(17):1529 – 1533, 2017. ISSN 0375-9601. doi: <https://doi.org/10.1016/j.physleta.2017.03.005>. URL <http://www.sciencedirect.com/science/article/pii/S0375960117302293>.
 26. Nzar Rauf Abdullah, Rawezh Bakr Marif, and Hunar Omar Rashid. Photon-mediated thermoelectric and heat currents through a resonant quantum wire-cavity system. *Energies*, 12(6), 2019. ISSN 1996-1073. doi: 10.3390/en12061082. URL <http://www.mdpi.com/1996-1073/12/6/1082>.
 27. Nzar Rauf Abdullah. Optical control of spin-dependent thermal transport in a quantum ring. *Physics Letters A*, 382(21):1432–1436, 2018. ISSN 0375-9601. doi: 10.1016/j.physleta.2018.03.042. URL <http://www.sciencedirect.com/science/article/pii/S0375960118303177>.
 28. Edward McCann and Mikito Koshino. The electronic properties of bilayer graphene. *Reports on Progress in Physics*, 76(5):056503, apr 2013. doi: 10.1088/0034-4885/76/5/056503. URL <https://doi.org/10.1088/0034-4885/76/5/056503>.
 29. M. Houmad, H. Zaari, A. Benyoussef, A. El Kenz, and H. Ez-Zahraouy. Optical conductivity enhancement and band gap opening with silicon doped graphene. *Carbon*, 94:1021–1027, 2015. ISSN 0008-6223. URL <http://www.sciencedirect.com/science/article/pii/S0008622315300567>.
 30. S. J. Zhang, S. S. Lin, X. Q. Li, X. Y. Liu, H. A. Wu, W. L. Xu, P. Wang, Z. Q. Wu, H. K. Zhong, and Z. J. Xu. Opening the band gap of graphene through silicon doping for the improved performance of graphene/gaas heterojunction solar cells. *Nanoscale*, 8:226–232, 2016. doi: 10.1039/C5NR06345K. URL <http://dx.doi.org/10.1039/C5NR06345K>.
 31. Hunar Omar Rashid, Nzar Rauf Abdullah, and Vidar Gudmundsson. Silicon on a graphene nanosheet with triangle- and dot-shape: Electronic structure, specific heat, and thermal conductivity from first-principle calculations. *Results in Physics*, 15:102625, 2019. ISSN 2211-3797. doi: 10.1016/j.rinp.2019.102625. URL <http://www.sciencedirect.com/science/article/pii/S2211379719317140>.
 32. Nzar Rauf Abdullah, Chi-Shung Tang, Andrei Manolescu, and Vidar Gudmundsson. The photocurrent generated by photon replica states of an off-resonantly coupled dot-cavity system. *Scientific Reports*, 9(1):14703, 2019. ISSN 2045-2322. doi: 10.1038/s41598-019-51320-8. URL <https://doi.org/10.1038/s41598-019-51320-8>.
 33. Aziz H. Fatah, R.A. Radhi, and Nzar R. Abdullah. Analytical derivations of single-particle matrix elements in nuclear shell model. *Communications in Theoretical Physics*, 66(1):104–114, jul 2016. doi: 10.1088/0253-6102/66/1/104. URL <https://doi.org/10.1088/0253-6102/66/1/104>.
 34. Nzar Rauf Abdullah, Chi-Shung Tang, Andrei Manolescu, and Vidar Gudmundsson. Manifestation of the purcell effect in current transport through a dot-cavity-qed system. *Nanomaterials*, 9(7):1023, 2019.
 35. Nzar Rauf Abdullah, Chi-Shung Tang, Andrei Manolescu, and Vidar Gudmundsson. Cavity-photon-switched coherent transient transport in a double quantum waveguide. *Journal of Applied Physics*, 116(23):233104, 2014. doi: 10.1063/1.4904907. URL <https://doi.org/10.1063/1.4904907>.
 36. Chi-Shung Tang, Yun-Hsuan Yu, Nzar Rauf Abdullah, and Vidar Gudmundsson. Transport signatures of top-gate bound states with strong rashba-zeeman effect. *Physics Letters A*, 381(47):3960 – 3963, 2017. ISSN 0375-9601. doi: <https://doi.org/10.1016/j.physleta.2017.10.012>. URL <http://www.sciencedirect.com/science/article/pii/S0375960117309684>.
 37. Nzar Rauf Abdullah, Chi-Shung Tang, Andrei Manolescu, and Vidar Gudmundsson. Oscillations in electron transport caused by multiple resonances in a quantum dot-qed system in the steady-state regime. *Physica E: Low-dimensional Systems and Nanostructures*, 123:114221, 2020. ISSN 1386-9477. doi: <https://doi.org/10.1016/j.physe.2020.114221>. URL <http://www.sciencedirect.com/science/article/pii/S1386947719311750>.
 38. John P. Perdew, Kieron Burke, and Matthias Ernzerhof. Generalized gradient approximation made simple. *Phys. Rev. Lett.*, 77:3865–3868, Oct 1996. doi: 10.1103/PhysRevLett.77.3865. URL <https://link.aps.org/doi/10.1103/PhysRevLett.77.3865>.
 39. Paolo Giannozzi, Stefano Baroni, Nicola Bonini, Matteo Calandra, Roberto Car, Carlo Cavazzoni, Davide Ceresoli, Guido L Chiarotti, Matteo Cococcioni, Ismaila Dabo, Andrea Dal Corso, Stefano de Gironcoli, Stefano Fabris, Guido Fratesi, Ralph Gebauer, Uwe Gerstmann, Christos Gougousis, Anton Kokalj, Michele Lazzeri, Layla Martin-Samos, Nicola Marzari, Francesco Mauri, Riccardo Mazzarello, Stefano Paolini, Alfredo Pasquarello, Lorenzo Paulatto, Carlo Sbraccia, Sandro Scandolo, Gabriele Sclauzero, Ari P Seitsonen, Alexander Smogunov, Paolo Umari, and Renata M Wentzcovitch. QUANTUM ESPRESSO: a modular and open-source software project for quantum simulations of materials. *Journal of Physics: Condensed Matter*, 21(39):395502, sep 2009. doi: 10.1088/0953-8984/21/39/395502. URL <https://doi.org/10.1088/0953-8984/21/39/395502>.
 40. J. P. Perdew and Alex Zunger. Self-interaction correction to density-functional approximations for many-electron systems. *Phys. Rev. B*, 23:5048–5079, May 1981. doi: 10.1103/PhysRevB.23.5048. URL <https://link.aps.org/doi/10.1103/PhysRevB.23.5048>.
 41. Anton Kokalj. Xcrysden—a new program for displaying crystalline structures and electron densities. *Journal of Molecular Graphics and Modelling*, 17(3):176–179, 1999. ISSN 1093-3263. doi: 10.1016/S1093-3263(99)00028-5. URL <http://www.sciencedirect.com/science/article/pii/S1093326399000285>.
 42. Nzar Rauf Abdullah, Aziz H Fatah, and Jabar M A Fatah. Effects of magnetic field on photon-induced quantum transport in a single dot-cavity system. *Chinese Physics B*, 25(11):114206,

2016. URL <http://stacks.iop.org/1674-1056/25/i=11/a=114206>.
43. Georg KH Madsen and David J Singh. Boltztrap, a code for calculating band-structure dependent quantities. *Computer Physics Communications*, 175(1):67–71, 2006.
 44. Nzar Rauf Abdullah, Gullan Ahmed Mohammed, Hunar Omar Rashid, and Vidar Gudmundsson. Electronic, thermal, and optical properties of graphene like sixc structures: Significant effects of si atom configurations. *Physics Letters A*, 384(24):126578, 2020. ISSN 0375-9601. doi: <https://doi.org/10.1016/j.physleta.2020.126578>. URL <http://www.sciencedirect.com/science/article/pii/S037596012030445X>.
 45. Nzar Rauf Abdullah, Chi-Shung Tang, Andrei Manolescu, and Vidar Gudmundsson. The interplay of electron-photon and cavity-environment coupling on the electron transport through a quantum dot system. *Physica E: Low-dimensional Systems and Nanostructures*, 119:113996, 2020. ISSN 1386-9477. doi: <https://doi.org/10.1016/j.physe.2020.113996>. URL <http://www.sciencedirect.com/science/article/pii/S1386947719312445>.
 46. Nzar Rauf Abdullah. Rabi-resonant and intraband transitions in a multilevel quantum dot system controlled by the cavity-photon reservoir and the electron-photon coupling. *Results in Physics*, 15:102686, 2019. ISSN 2211-3797. doi: <https://doi.org/10.1016/j.rinp.2019.102686>. URL <http://www.sciencedirect.com/science/article/pii/S221137971932251X>.
 47. Thorsteinn H. Jonsson, Andrei Manolescu, Hsi-Sheng Goan, Nzar Rauf Abdullah, Anna Sitek, Chi-Shung Tang, and Vidar Gudmundsson. Efficient determination of the markovian time-evolution towards a steady-state of a complex open quantum system. *Computer Physics Communications*, 220:81 – 90, 2017. ISSN 0010-4655. doi: <https://doi.org/10.1016/j.cpc.2017.06.018>. URL <http://www.sciencedirect.com/science/article/pii/S001046551730200X>.
 48. Pengfei Li, Rulong Zhou, and Xiao Cheng Zeng. The search for the most stable structures of silicon-carbon monolayer compounds. *Nanoscale*, 6(20):11685–11691, 2014. ISSN 2040-3364. doi: <https://doi.org/10.1039/C4NR03247K>. URL <http://dx.doi.org/10.1039/C4NR03247K>.
 49. Nzar Rauf Abdullah, Hunar Omar Rashid, Andrei Manolescu, and Vidar Gudmundsson. Interlayer interaction controlling the properties of ab- and aa-stacked bilayer graphene-like bc14n and si2c14. *Surfaces and Interfaces*, 21:100740, 2020. ISSN 2468-0230. doi: <https://doi.org/10.1016/j.surfin.2020.100740>. URL <http://www.sciencedirect.com/science/article/pii/S246802302030732X>.
 50. Jae-Kap Lee, Seung-Cheol Lee, Jae-Pyoung Ahn, Soo-Chul Kim, John I. B. Wilson, and Phillip John. The growth of aa graphite on (111) diamond. *The Journal of Chemical Physics*, 129(23):234709, 2008. doi: <https://doi.org/10.1063/1.2975333>. URL <https://doi.org/10.1063/1.2975333>.
 51. Nzar Rauf Abdullah, Chi-Shung Tang, and Vidar Gudmundsson. Time-dependent magnetotransport in an interacting double quantum wire with window coupling. *Phys. Rev. B*, 82:195325, Nov 2010. doi: <https://doi.org/10.1103/PhysRevB.82.195325>. URL <https://link.aps.org/doi/10.1103/PhysRevB.82.195325>.
 52. Vidar Gudmundsson, Nzar Rauf Abdullah, Chi-Shung Tang, Andrei Manolescu, and Valeriu Moldoveanu. Cavity-photon-induced high-order transitions between ground states of quantum dots. *Annalen der Physik*, 531(11):1900306, 2019. doi: <https://doi.org/10.1002/andp.201900306>. URL <https://onlinelibrary.wiley.com/doi/abs/10.1002/andp.201900306>.
 53. Nzar Rauf Abdullah, Hunar Omar Rashid, Andrei Manolescu, and Vidar Gudmundsson. Interlayer interaction controlling the properties of ab- and aa-stacked bilayer graphene-like bc₁₄n and si₂c₁₄. *arXiv preprint arXiv:2008.10888*, 2020.
 54. Vidar Gudmundsson, Anna Sitek, Pei-yi Lin, Nzar Rauf Abdullah, Chi-Shung Tang, and Andrei Manolescu. Coupled collective and rabi oscillations triggered by electron transport through a photon cavity. *ACS Photonics*, 2(7):930–934, 2015. doi: <https://doi.org/10.1021/acsp Photonics.5b00115>. URL <https://doi.org/10.1021/acsp Photonics.5b00115>.
 55. Nzar Rauf Abdullah, Hunar Omar Rashid, Chi-Shung Tang, Andrei Manolescu, and Vidar Gudmundsson. Properties of bsi₆n monolayers derived by first-principle computation. *arXiv preprint arXiv:2008.03782*, 2020.
 56. Vidar Gudmundsson, Thorsteinn H. Jonsson, Maria Laura Bernodsson, Nzar Rauf Abdullah, Anna Sitek, Hsi-Sheng Goan, Chi-Shung Tang, and Andrei Manolescu. Regimes of radiative and nonradiative transitions in transport through an electronic system in a photon cavity reaching a steady state. *Annalen der Physik*, 529(1-2):1600177, 2017. doi: <https://doi.org/10.1002/andp.201600177>. URL <https://onlinelibrary.wiley.com/doi/abs/10.1002/andp.201600177>.
 57. Nzar Rauf Abdullah, Chi-Shung Tang, Andrei Manolescu, and Vidar Gudmundsson. Competition of static magnetic and dynamic photon forces in electronic transport through a quantum dot. *Journal of Physics: Condensed Matter*, 28(37):375301, jul 2016. doi: <https://doi.org/10.1088/0953-8984/28/37/375301>. URL <https://doi.org/10.1088/0953-8984/28/37/375301>.
 58. Vidar Gudmundsson, Nzar Rauf Abdulla, Anna Sitek, Hsi-Sheng Goan, Chi-Shung Tang, and Andrei Manolescu. Electroluminescence caused by the transport of interacting electrons through parallel quantum dots in a photon cavity. *Annalen der Physik*, 530(2):1700334, 2018. doi: <https://doi.org/10.1002/andp.201700334>. URL <https://onlinelibrary.wiley.com/doi/abs/10.1002/andp.201700334>.
 59. Junfeng Zhang and Jijun Zhao. Mechanical properties of bilayer graphene with twist and grain boundaries. *Journal of Applied Physics*, 113(4):043514, 2013. doi: <https://doi.org/10.1063/1.4789594>. URL <https://doi.org/10.1063/1.4789594>.
 60. Changgu Lee, Xiaoding Wei, Jeffrey W. Kysar, and James Hone. Measurement of the elastic properties and intrinsic strength of monolayer graphene. *Science*, 321(5887):385–388, 2008. ISSN 0036-8075. doi: <https://doi.org/10.1126/science.1157996>. URL <https://science.sciencemag.org/content/321/5887/385>.
 61. X K Lu, T Y Xin, Q Zhang, Q Xu, T H Wei, and Y X Wang. Versatile mechanical properties of novel g-SiC_x monolayers from graphene to silicene: a first-principles study. *Nanotechnology*, 29(31):315701, may 2018. doi: <https://doi.org/10.1088/1361-6528/aac337>. URL <https://doi.org/10.1088/1361-6528/aac337>.
 62. Vidar Gudmundsson, Nzar Rauf Abdullah, Anna Sitek, Hsi-Sheng Goan, Chi-Shung Tang, and Andrei Manolescu. Current correlations for the transport of interacting electrons through parallel quantum dots in a photon cavity. *Physics Letters A*, 382(25):1672 – 1678, 2018. ISSN 0375-9601. doi: <https://doi.org/10.1016/j.physleta.2018.04.017>. URL <http://www.sciencedirect.com/science/article/pii/S0375960118303748>.
 63. Mahmood Aliofkhaezrai, Nasar Ali, William I Milne, Cengiz S Ozkan, Stanislaw Mitura, and Juana L Gervasoni. *Graphene Science Handbook: Nanostructure and Atomic Arrangement*. CRC Press, 2016.
 64. Vidar Gudmundsson, Anna Sitek, Nzar Rauf Abdullah, Chi-Shung Tang, and Andrei Manolescu. Cavity-photon contribution to the effective interaction of electrons in parallel quantum dots. *Annalen der Physik*, 528(5):394–403, 2016. doi: <https://doi.org/10.1002/andp.201500298>. URL <https://onlinelibrary.wiley.com/doi/abs/10.1002/andp.201500298>.
 65. Gul Rahman. Distortion and electric-field control of the band structure of silicene. *EPL (Europhysics Letters)*, 105(3):37012, feb 2014. doi: <https://doi.org/10.1209/0295-5075/105/37012>. URL <https://doi.org/10.1209/0295-5075/105/37012>.
 66. Nzar Rauf Abdullah, Chi-Shung Tang, Andrei Manolescu, and Vidar Gudmundsson. Cavity-photon controlled thermoelectric transport through a quantum wire. *ACS Photonics*, 3(2):249–254, 2016. doi: <https://doi.org/10.1021/acsp Photonics.5b00532>. URL <https://doi.org/10.1021/acsp Photonics.5b00532>.
 67. Nzar Rauf Abdullah, Chi-Shung Tang, Andrei Manolescu, and Vidar Gudmundsson. Spin-dependent heat and thermoelectric currents in a rashba ring coupled to a photon cavity. *Physica E: Low-dimensional Systems and Nanostructures*, 95:102 – 107, 2018. ISSN 1386-9477. doi: <https://doi.org/10.1016/j.physe.2017.09.011>. URL <http://www.sciencedirect.com/science/article/pii/S1386947717311372>.
 68. Nzar Rauf Abdullah, Thorsten Arnold, Chi-Shung Tang, Andrei Manolescu, and Vidar Gudmundsson. Photon-induced tunability of the thermospin current in a rashba ring. *Journal of Physics: Condensed Matter*, 30(14):145303, mar 2018. doi: <https://doi.org/10.1088/1361-648x/aab255>. URL <https://doi.org/10.1088/1361-648x/aab255>.
 69. S. Yiğen, V. Tayari, J. O. Island, J. M. Porter, and A. R. Champagne. Electronic thermal conductivity measurements in intrinsic graphene. *Phys. Rev. B*, 87:241411, Jun 2013. doi: <https://doi.org/10.1103/PhysRevB.87.241411>. URL <https://link.aps.org/doi/10.1103/PhysRevB.87.241411>.
 70. Palash Nath, D. Sanyal, and Debnarayan Jana. Ab-initio calculation of optical properties of aa-stacked bilayer graphene with tunable layer separation. *Current Applied Physics*, 15(6):691 – 697, 2015. ISSN 1567-1739. doi: <https://doi.org/10.1016/j.cap.2015.03.011>. URL <http://www.sciencedirect.com/science/article/pii/S1567173915000887>.
 71. Brij Mohan, Ashok Kumar, and P.K. Ahluwalia. A first principle study of interband transitions and electron energy loss in mono and bilayer graphene: Effect of external electric field. *Physica E: Low-dimensional Systems and Nanostructures*, 44(7):1670 – 1674, 2012. ISSN 1386-9477. doi: <https://doi.org/10.1016/j.physe.2012.03.011>.

- physe.2012.04.017. URL <http://www.sciencedirect.com/science/article/pii/S1386947712001634>.
72. Vidar Gudmundsson, Nzar Rauf Abdullah, Chi-Shung Tang, Andrei Manolescu, and Valeriu Moldoveanu. Cavity-photon-induced high-order transitions between ground states of quantum dots. *Annalen der Physik*, 531(11):1900306, 2019. doi: 10.1002/andp.201900306. URL <https://onlinelibrary.wiley.com/doi/abs/10.1002/andp.201900306>.
 73. N R Abdullah, C S Tang, A Manolescu, and V Gudmundsson. Delocalization of electrons by cavity photons in transport through a quantum dot molecule. *Physica E*, 64:254–262, 2014.
 74. Nzar Rauf Abdullah, Chi-Shung Tang, Andrei Manolescu, and Vidar Gudmundsson. Coherent transient transport of interacting electrons through a quantum waveguide switch. *Journal of Physics: Condensed Matter*, 27(1):015301, nov 2014. doi: 10.1088/0953-8984/27/1/015301. URL <https://doi.org/10.1088/0953-8984/27/1/015301>.